doi:10.36487/ACG_repo/2063_13

Back analysis of the effect of hydraulic fracturing preconditioning on mining-induced seismicity at the main access of New Mine Level project, CODELCO Chile - El Teniente Division

E Ghazvinian Itasca Consulting Group, United States

B Damjanac Itasca Consulting Group, United States

L Lorig Itasca Consulting Group, United States

P Cavieres CODELCO, Chile

A Madrid CODELCO, Chile

Abstract

CODELCO has been using hydraulic fracturing (HF) to precondition rock masses at El Teniente Mine. There are indications that HF preconditioning is effective in controlling mining-induced seismicity around the current infrastructure and may also provide other mining benefits (e.g., caveability) elsewhere. The initial excavation of Túnel Acceso Personal (TAP) to the New Mine Level experienced frequent and relatively strong seismic activity. To reduce the seismic hazard during continued TAP excavation, the mine carried out HF preconditioning of the rock mass along the projected tunnel alignment before tunnel advance. Reduced maximum seismic event magnitude was observed for the preconditioned rock mass during tunnel advance when compared to un-preconditioned rock. This paper discusses the use of a distinct element numerical modeling code, 3DEC, to analyze the HF preconditioning trial and numerically demonstrate the effect of HF preconditioning on the reduction of mining-induced seismic hazard. In particular, it addresses the calibration process to numerically reproduce the seismic catalog associated with HF preconditioning and tunnel advance in the preconditioned rock mass. Subsequently, the model was used to compare mining-induced seismicity in the preconditioned and un-preconditioned rock masses. Back analysis of this experiment by means of coupled hydro-mechanical models provided further insight into the mechanics of HF preconditioning and its use as a tool for reducing and controlling mining-induced seismicity. One mechanism that can cause seismicity during HF and reduce the potential for subsequent mining-induced seismicity is the interaction between the hydraulic fracture and the discrete fracture network (DFN), resulting in "hydro-shearing" on pre-existing fractures caused by fluid leakoff from the main hydraulic fracture. The importance of hydro-shearing in successful application of HF treatment in reducing the mining-induced seismic hazard during the TAP advance is discussed based on observations from the calibrated numerical model.

1 Introduction

The New Mine Level (NML) project is being planned to extend the life of El Teniente Mine by expanding mining operation deeper, approximately 100 m below the existing main haulage level of the mine, putting the NML at about 1,000 m depth. A significant component of the NML development is construction of the two main access tunnels: a "horse-shoe" shaped tunnel for access of personnel (Túnel Acceso Personal or TAP) and a twin conveyor tunnel for ore transport. The two parallel tunnels are approximately 9 km in length and 8 m in diameter. The TAP dips approximately 5° from the horizontal plane with azimuth of ~237°. The initial excavation of TAP has been associated with frequent and relatively strong seismic activity. Seismic events up to a magnitude of Mw 2.6 were recorded. Those events can be attributed to a combination of high overburden stress and TAP alignment intersecting a complex geological environment characterized

by rock variability: from igneous (effusive and intrusive) to sedimentary volcanoclastic rocks, with sectors of intense hydrothermal alteration (Verzani et al. 2015). Hydraulic fracturing (HF) preconditioning of the rock mass along the projected tunnel alignment prior to tunnel advance was proposed to manage the seismic hazard during continued TAP excavation based on CODELCO's preconditioning experience at El Teniente.

CODELCO initiated studies on preconditioning of the rock mass by hydraulic fracturing (HF) at El Teniente in 2004. The application of HF technique was carried out in the Diablo Regimiento sector. The purpose of the experiment was to evaluate the technical viability of preconditioning using HF (considering the mine is operated under high in-situ stress conditions) and to potentially reduce the hazard of inducing rockburst events. The results are documented by Morales et al. (2007). The tonnage involved in the volume of preconditioned ground was 3.87 Mt. The hydraulic fractures were generated at a vertical spacing of 1.5 m. The fractures have been estimated to be approximately circular with a 40 m diameter. The test successfully reduced seismicity, as shown in Figure 1. There were indications that, among other potential benefits (e.g., caveability), the HF preconditioning provided a means of controlling mining-induced seismicity near the current infrastructure.

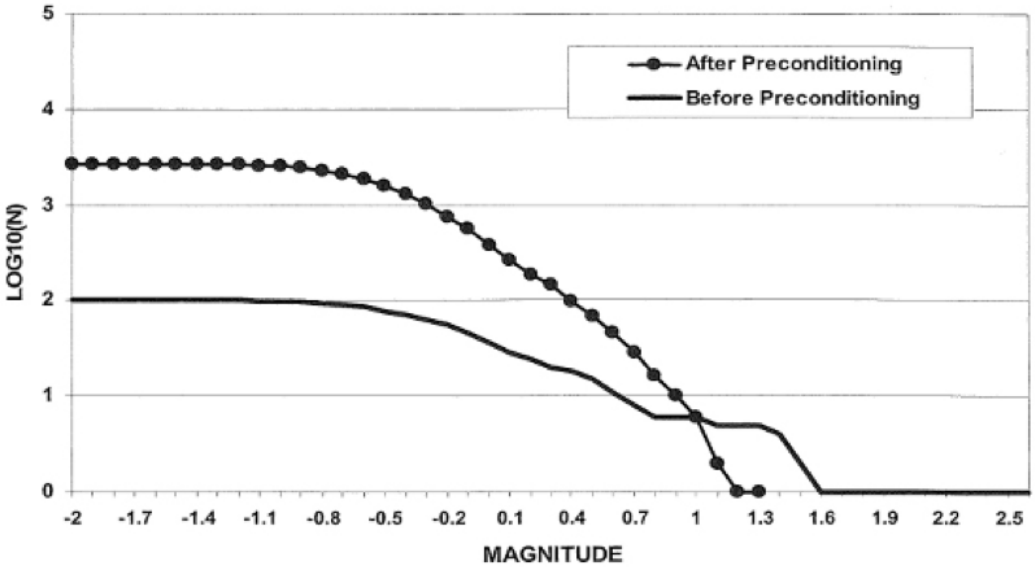

Figure 1 Seismic behavior before and after application of hydraulic fracturing (Morales et al. 2007)

Hydraulic fracturing of the rock mass ahead of the TAP segment that was initially excavated in highly stressed ground was carried out from four boreholes (denominated BH10, BH20, BH30, and BH40). The relative location of the boreholes to the TAP advance alignment is shown in Figure 2. The advance of the TAP in preconditioned rock mass was associated with seismic events significantly smaller (less than 1 Mw) than events recorded during excavation of the TAP in un-preconditioned ground. This indicated that HF preconditioning effectively reduced mining-induced seismic hazard, specifically the magnitude of the largest seismic events.

Given the successful HF preconditioning trial, the mine initiated a numerical study to investigate the mechanisms and quantify reduction of seismic hazard along the TAP. It is not clear if HF at deeper levels with greater in-situ stresses would be as beneficial as it appears to be for the current mining. Robust and physics-based numerical models capable of explicitly representing discrete fractures and their effect on deformation (including seismic slip) and failure of rock mass as well as pore pressure dissipation into the rock mass allow for a relatively quick analysis of the effect of HF preconditioning on mining-induced seismicity. The overall objectives of this study were to: 1) understand the mechanics of how preconditioning of the TAP is effectively reducing mining-induced seismicity; 2) quantify the reduction of seismic hazard along the TAP by HF preconditioning; and 3) develop a calibrated model to use as a predictive tool for examining the efficiency of future HF designs in the TAP, and for other locations using previous specific validated/calibrated numerical models.

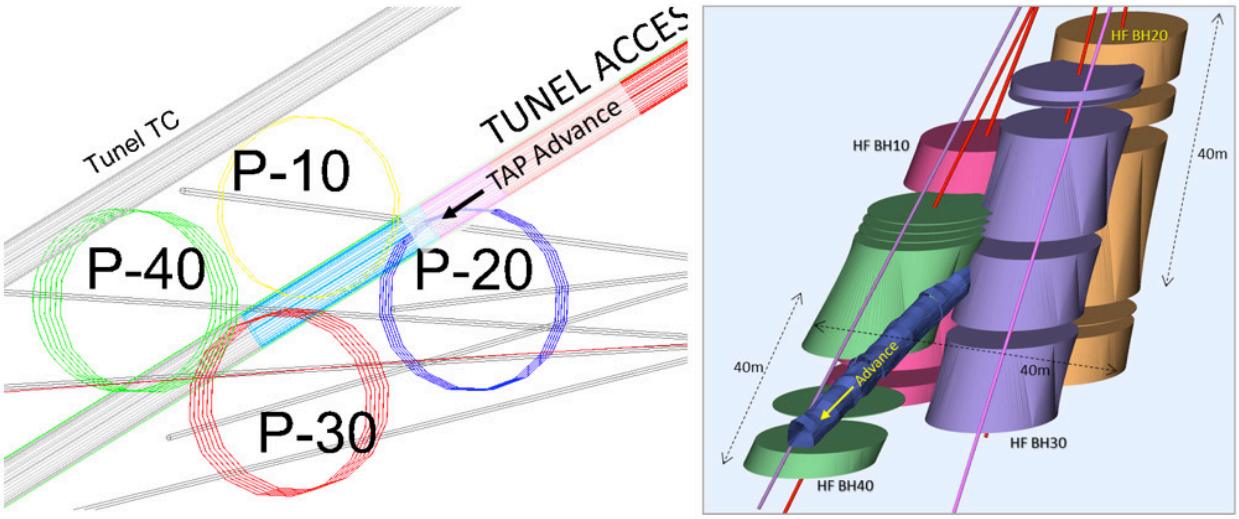

Figure 2 Relative location of preconditioning boreholes to the TAP (courtesy of CODELCO)

2 Numerical approach

A detailed back-analysis of the completed HF preconditioning and the TAP advance at El Teniente Mine was carried out using the distinct element numerical code 3DEC (Itasca 2015). Discrete hydraulic fractures and entire discrete fracture networks (DFNs), including thousands of finite-size fractures (e.g., circular disks) can be explicitly represented in 3DEC in both the mechanical and flow models. Mechanically, fractures can slip and open as a function of effective stress and their strength. As fractures deform, the corresponding seismic response is computed based on instantaneous slip of the fractures. Synthetic seismic event locations, timing, magnitude, and mechanism are determined to create a synthetic seismic catalogue associated with the hydraulic fracture. In the flow model, each fracture acts as a fluid conduit, allowing simulation of flow through the DFN. The mechanical and flow models can be coupled at different levels, from a relatively simple effective stress calculation for a given pore pressure distribution, to a fully, two-way, coupled hydro-mechanical simulation.

Pore pressure dissipation within HF and into the DFN is numerically simulated in a fully coupled hydro-mechanical analysis. The explicit faults have different properties than the DFN, but are numerically treated as identical to the DFN in the model. The simulation predicts evolution of the injection pressure (including both initiation and propagation pressures) and evolution of the size of the hydraulic fracture. The fracture propagation is associated with fluid percolation into the DFN, change in the pore pressure, and deformation of the rock mass and DFN. Some of the DFN fractures slip seismically. The injection pressures and the pore pressure dissipation into the rock mass are calibrated by comparison with field data. The maximum seismic event magnitude is determined from the numerical results and compared with field data. The model is calibrated by adjusting the uncertain model parameters until the numerical results compare reasonably well with field data.

The fully coupled hydro-mechanical simulation provides accurate results for HF simulation but is not practical in terms of computational run time to simulate preconditioning of a rock mass as detailed as individual injections along multiple boreholes. For this reason, a hybrid approach was adopted in this study, whereby a generalized rule for pressure changes in the vicinity of individual injection points was established from fully coupled hydro-mechanical models (referred to as "local coupled models" in this paper – Section 3). The generalized rule was then applied in global models (Section 4) as a means to precondition the rock mass along the boreholes by defining pore pressure distribution in the HF, DFN, and faults (effective stress calculation), followed by TAP excavation.

2.1 Discrete Fracture Network (DFN)

A Discrete Fracture Network (DFN) generated in 3DEC represented veinlets or fractures that were mapped as discontinuities. The fracture sets are listed in Table 1. A preliminary effective stress analysis identified

Fracture Sets 3 and 4 as the most critically oriented fractures for hydro-shearing (Blanksma et al. 2018). On the other hand, fractures in Set 2 are oriented least favorably with respect to the in-situ stress for hydro-shearing. Therefore, a simplified DFN with approximately 1,150 fractures was created by bootstrapping fracture sizes in a 200×200×150 m volume consistent with the 3DEC model domain and placed uniformly throughout the domain (Figure 3). The DFN combines Fracture Set 2 with Fracture Set 4 for calculation runtime efficiency (therefore, Set 2 is not listed in Table 1). Additionally, fifty deterministic faults mapped explicitly were added to the 3DEC model.

Table 1 Properties used to generate DFN

Fracture Set	Property	Distribution	Parameters
Set 1	Position	Uniform	Positions generated in the model domain
	Orientation*	Fisher	Dip = 79°, Dip Direction = 70°, κ = 200
	Size (Radius)	Bootstrapped	Fracture size from seismic data, l_{min} = 0.3, l_{max} = 100
	Density		P_{32} = 1.8 in the model domain
Set 3	Position	Uniform	Positions generated in the model domain
	Orientation	Fisher	Dip = 30°, Dip Direction = 79°, κ = 200
	Size (Radius)	Bootstrapped	Fracture size from seismic data, l_{min} = 0.3, l_{max} = 100
	Density		P_{32} = 1.0 in the model domain
Set 4	Position	Uniform	Positions generated in the model domain
	Orientation	Fisher	Dip = 45° in this study, Dip Direction = 176°, κ = 200
	Size (Radius)	Bootstrapped	Fracture size from seismic data, l_{min} = 0.3, l_{max} = 100
	Density		P_{32} = 0.6 in the model domain
* Dip direction measured clockwise from north.			

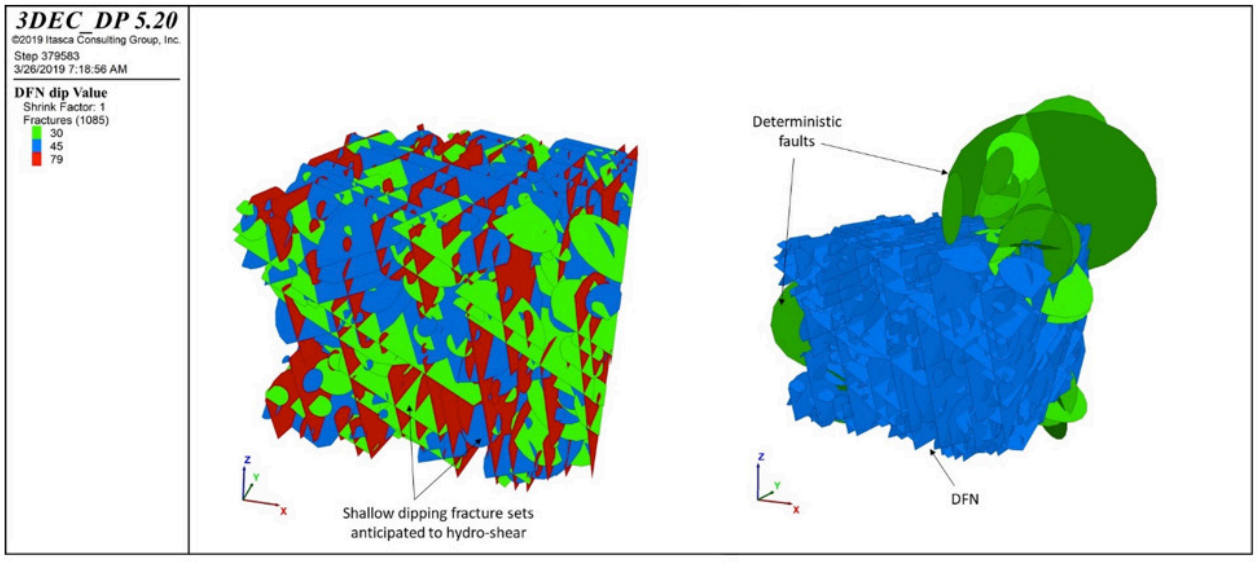

Figure 3 Simplifed DFN used in the numerical model

2.2 In-situ stress

The in-situ stresses are listed in Table 2. The magnitude of σ_3 is calibrated within acceptable limits according to the stress model for the mine to match the propagation pressure measured in the field.

Table 2 Principal stresses used in numerical model

Principal Stress	Dip Direction* (°)	Dip** (°)	Magnitude (MPa)
σ1	160.0	1.28	63.5
σ2	250.0	10.0	38.0
σ3	62.5	80.0	28.0

* Dip direction measured clockwise from north

** Dip measured positive downwards

2.3 Material properties

The rock mass in the model comprised a single rock type (CMET lithology, Complejo Máfico El Teniente) and was considered to behave in a linear elastic manner, with properties shown in Table 3.

Table 3 Rock mass properties used in numerical model

Name	Young's Modulus (GPa)	Poisson's Ratio	Density (kg/m^3)
CMET	50	0.25	2,700

Discontinuity properties were given different values for each type (with "discontinuity" referring to natural fractures, veinlets, HF, and faults). Similar properties were given to different Fracture Sets within the DFN. The calibrated discontinuity properties are listed in Table 4.

The initial values for stiffness, friction angle, cohesion, and tensile strengths for all discontinuities were determined from the available laboratory test data. The dilation angle was also chosen to be in the typical range for hard rocks. The apertures in the coupled model were back-calculated from the rough estimation of the rock mass permeability (10-8 m/s). All the above parameters were then refined through a calibration process. It was inferred from the calibration results that a dynamic friction angle must be used for discontinuities to reproduce large magnitude seismic events in the numerical models (Ghazvinian et al. 2019).

Table 4 Discontinuity properties used in numerical model (residual values in brackets)

Discontinuity Parameters	DFN	Deterministic Faults	HF
Normal Stiffness (GPa/m)	200	200	500
Shear Stiffness (GPa/m)	80	80	250
Static Friction Angle (°)	30	30	40
Dynamic Friction Angle (°)	15	15	15
Cohesion (MPa)	2.0 (0)	0 (0)	Infinite (0)
Tensile Strength (MPa)	0.1 (0)	0 (0)	0.1 (0)
Dilation Angle (°)	3	3	0
Initial Aperture (m) – for coupled model	1e-4	2e-4	1e-4
Maximum Aperture (m) – for coupled model	30e-4	30e-4	30e-4

The calibration process involved fine-tuning the discontinuity properties and the in-situ stress with one set of global properties to concurrently achieve the following:

- propagation pressure measured at injection points in the local coupled model consistent with field measurements;
- microseismic behavior in the local coupled injection model consistent with what was monitored at the mine during preconditioning;
- microseismic behavior in the global model during preconditioning consistent with what was monitored during field preconditioning; and
- microseismic behavior in the global model during advance of the TAP to be in agreement with what was observed during drift excavation before and after preconditioning.

Introduction of a scheme to mimic the drop of the discontinuity friction angle to its dynamic value at the onset of slipping and resetting it to the peak friction angle when slip stops was instrumental in successful calibration of capturing microseismic event magnitudes consistent with field measurements. Otherwise, it would not have been possible to have stable in-situ conditions and predict the observed event magnitudes during TAP advance in the same model. It has been observed in fault-slip events that the friction coefficient on discontinuity surfaces diminishes from static to its dynamic value at the onset of slipping as a function of slip velocity (Figure 4). Frictional strength is regained at the end of slip by the friction coefficient increasing back to its static value (see McGarr (1999) for more details).

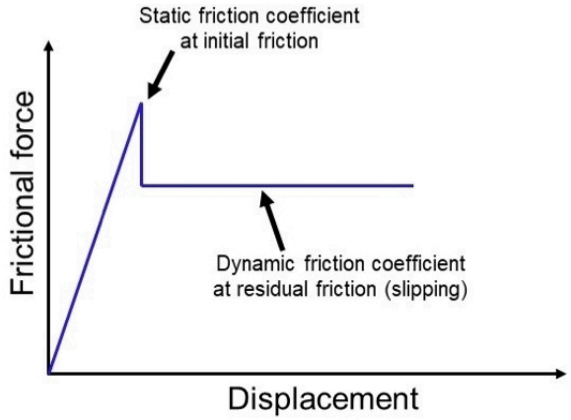

Figure 4 Schematic diagram of the frictional force as a function of displacement for a slip event

3 Local coupled model

In the local coupled model, fluid injection and pore pressure dissipation within HF and into the DFN and faults is numerically simulated in a fully coupled hydro-mechanical analysis for a series of statistically representative individual injection points. The simulation predicted evolution of the injection pressure (including both initiation and propagation pressures) and evolution of the size of the hydraulic fracture. The fracture propagation is associated with fluid percolation into the DFN, changes in the pore pressure, and deformation of the rock mass and DFN. Running this analysis for multiple consecutive injections at various spatial locations along one of the boreholes (i.e., BH10) allowed estimation of the combined response of the rock mass and DFN to HF treatment.

A cuboid model domain was constructed to be 200×200×150 m in size. Potential HF planes at injection locations were added to the 3DEC model as fractures perpendicular to the in-situ minimum principal stress. Those planes provide a potential pathway for the propagation of a hydraulic fracture (green lines in Figure 5).

Consecutive injections in two points along BH10 for a total duration of 3,600 seconds (1,800 seconds of injection time for each injection point) were performed. This allowed estimation of an overall response of the DFN to HF treatment as well as investigation of the effect of the remaining pore pressure in the DFN and faults from previous injections on pore pressure evolution of a propagating HF. In this analysis, the pore pressure in the first HF plane was nulled after injection completion and before injection into the second HF plane. This was done to mimic the behavior observed in a separate, more detailed model in which flow-back was simulated for 1,800 seconds after completion of injection. It was observed in that model that HF drains first into the borehole, long before the DFN and faults, practically trapping the fluid in those structures. The pore pressure in those structures dissipates slowly with insignificant change for 1,800 seconds, which is the average time between finishing and starting injection for two adjacent injection points.

An example of pore pressure evolution and stimulation of the critical fractures in the DFN for one set of consecutive injections is shown in Figure 6. It can be observed that with the second injection, the extent of stimulated fractures grows larger. The corresponding synthetic seismicity estimated from the average slip on discontinuities in the model is shown in Figure 7. The synthetic seismic data from the calibrated model covers the range of event magnitudes recorded during preconditioning.

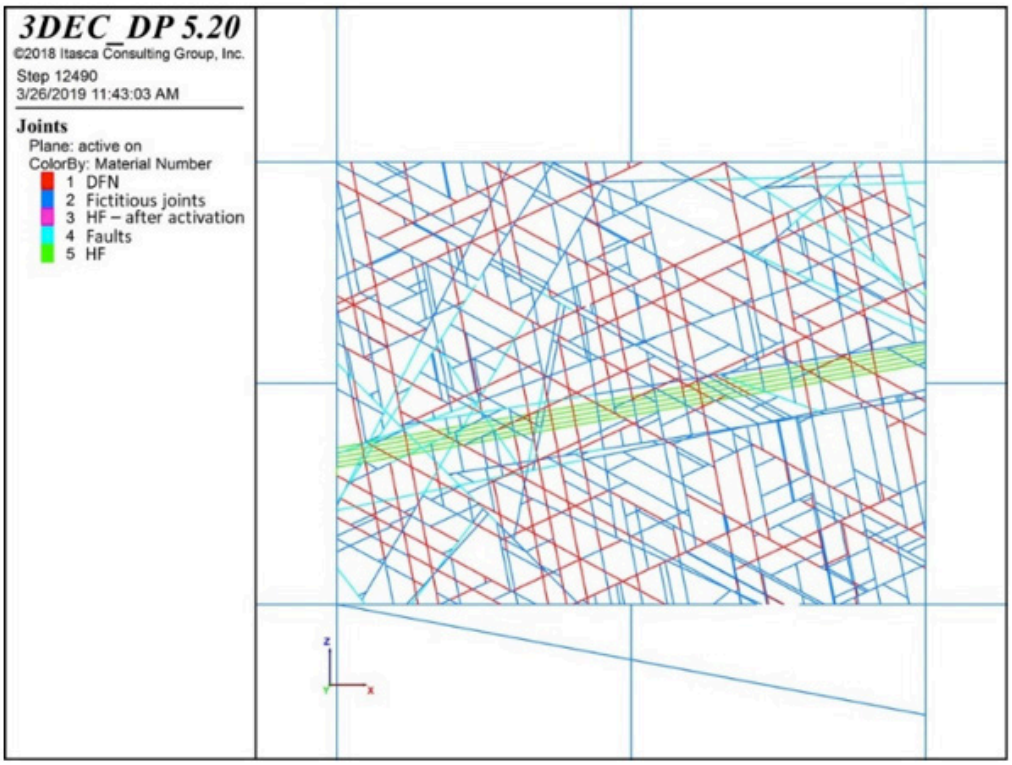

Figure 5 **Cut plane through the middle of the model showing different discontinuities (view looking model north)**

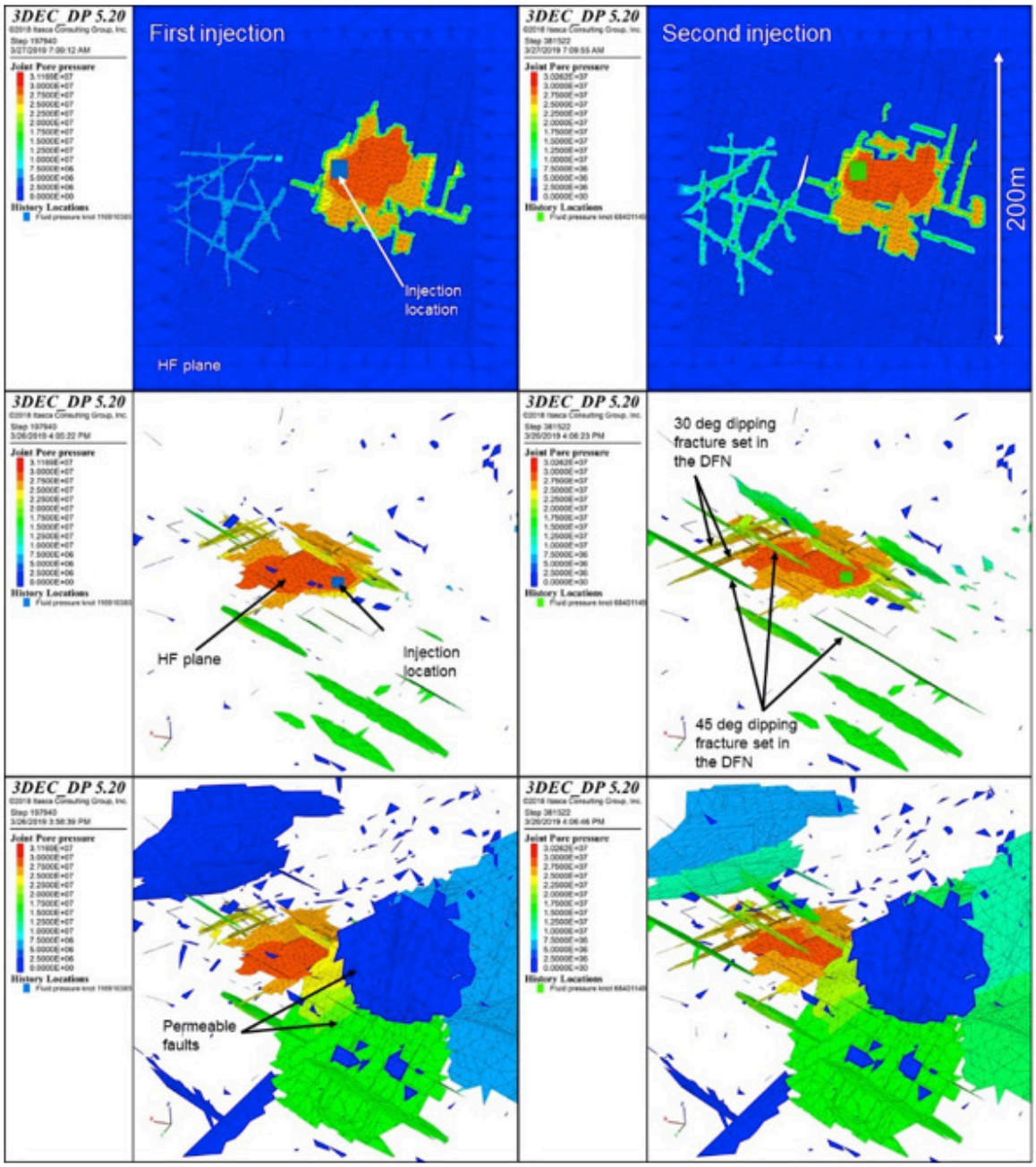

Figure 6 **Example of pore pressure (Pa) evolution in the HFs and DFN stimulation for two consecutive injections. The geometries of the induced hydraulic fractures are controlled by the intersecting faults and DFN fractures (y-axis is model north)**

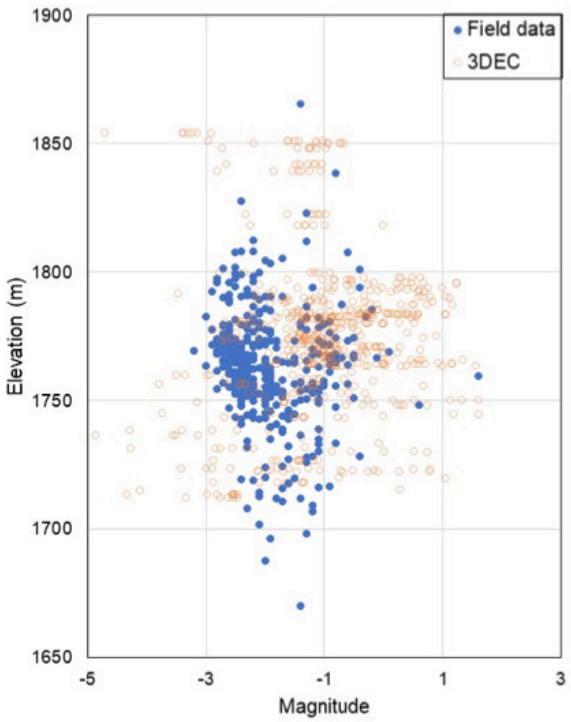

Figure 7 Comparison of synthetic microseismic data from an example 3DEC coupled model for two consecutive injections and seismic data recorded during HF treatment along BH10

By examining the extent of HF propagation and the volume of stimulated DFNs surrounding the injection locations, a generalization scheme for pore pressure initialization in the global model was inferred. For computational efficiency, the global model—which incorporates the HF treatment from the four boreholes as well as the drift advance—does not simulate HF propagation and fluid flow. Instead of running fully coupled hydro-mechanical simulation in the global model, the pore pressure changes due to hydraulic fracturing are imported into the model incrementally (i.e., increasing then decreasing the pore pressure for each hydraulic fracturing stage), and the global model is equilibrated for each pore pressure change. Thus, the effect of hydraulic fracturing is simulated in a more computationally efficient manner. Based on the results of the coupled injection models, pore pressures were initialized for the critical Fracture Sets (3 and 4) in the DFN, as well as faults and HF planes that fall within an ellipsoidal geometry bounding each injection location where pore pressures were observed to change in the coupled model:

- For DFN fractures and faults, the ellipsoid is defined by 70 m radius in the y-direction, 35 m radius in the xdirection, and 35 m radius in height.
- For HF planes, the ellipsoid is defined by 70 m radius in the y-direction, 35 m radius in the xdirection, and 5 m radius in height.

A pore pressure of 30 MPa is initialized for stimulation of DFN fractures and HF planes, and 25 MPa pore pressure is initialized for deterministic faults. These values were approximated from the developed pore pressure in the DFN fractures, faults, and HF planes near the injection points (e.g., Figure 6).

4 Global model

The global model was created with a similar domain size and identical DFN to the local model. A series of parallel HF planes were propagated across the domain with an approximate spacing of 2 m. Care was taken to ensure the generated HF planes in the model would cover the entire extent of the four injection holes. The “horse-shoe” shaped TAP is 8 m wide at the base and 8 m tall. Figure 8 shows the dimensions and layout of the 3DEC model in a vertical cross-section.

Prior to simulation of HF treatment in the global model, part of the drift that was mined before pre-conditioning was excavated (Figure 8). A synthetic microseismic event with magnitude of 2.1 was recorded, which is in close agreement with the largest event magnitudes recorded during actual advance of the TAP prior to preconditioning (largest event recorded is M 2.6).

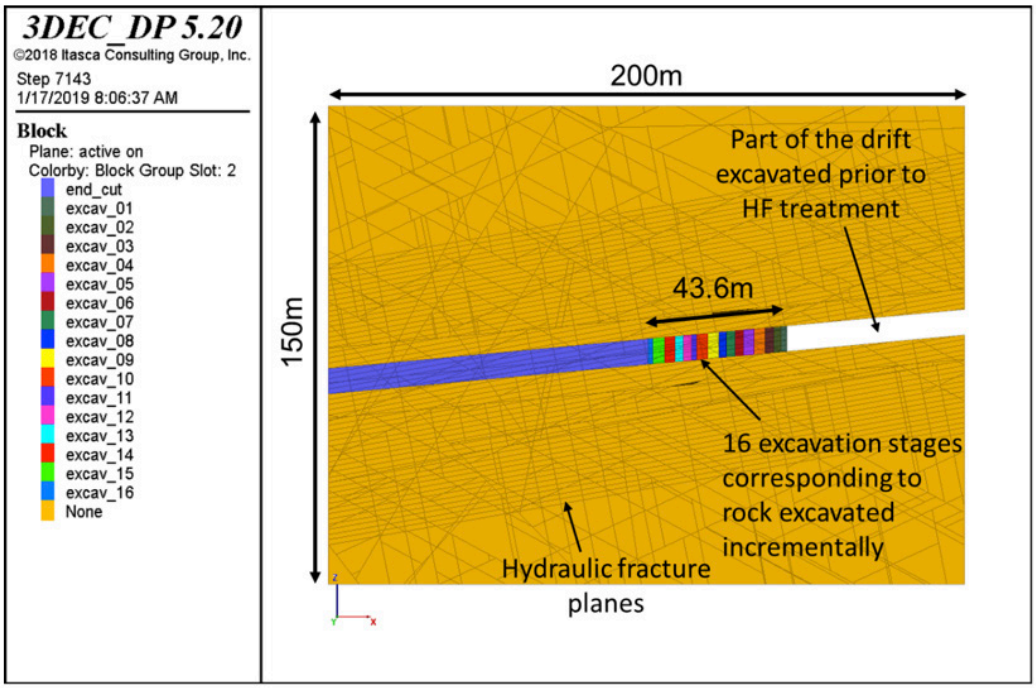

Figure 8 Geometry and staging of TAP advance simulation (view looking model north)

4.1 Preconditioning

The preconditioning along each borehole is simulated in four stages, as shown in Figure 9. Pore pressure initialization in the structures surrounding injection points belonging to each stage is performed gradually in 30 increments to avoid a numerically induced inertial effect. After completion of each borehole, the pore pressure is dropped to zero for the entire model, which is also done in 30 increments. For initialization of the pore pressure in the model, the generalization scheme that was inferred from the local model was used. Two cases of preconditioning were simulated: one with pore pressure initialized in the DFN (critical Fracture Sets), faults, and HF planes, and another with pore pressure initialized in HF planes only. Although the local model shows mobilization of critical fracture sets and faults, the model with stimulation of HF planes only was simulated to investigate the importance of stress relief in the fractures and faults. In other words, this model was used to investigate if shear stress release in the DFN and faults can be achieved if fluid does not percolate into, and pore pressure does not increase in, the DFN and faults. The stimulated contacts using the generalized scheme for the DFN, faults, and HF planes at different stages of preconditioning are shown in Figure 10.

Comparison of the synthetic seismicity recorded during pore pressure initialization along BH10 in the global model with the events recorded during preconditioning from BH10 showed good agreement. This confirms the quality of the model calibration and increases confidence in the synthetic microseismic data recorded during the TAP advance in the global model.

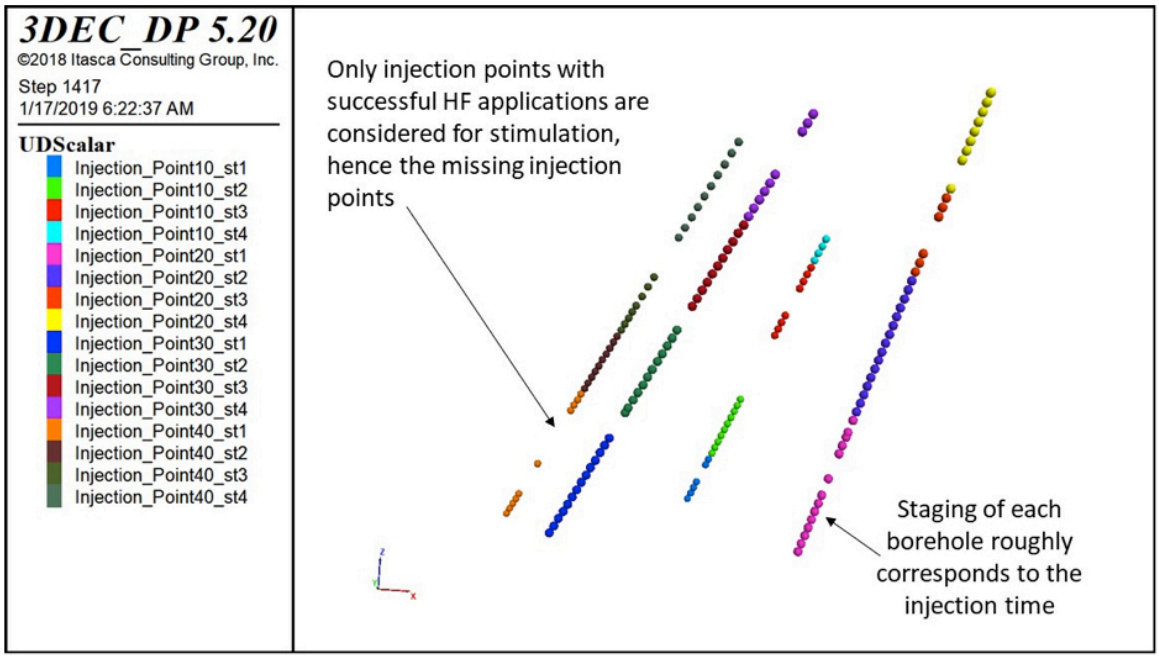

Figure 9 Staging of preconditioning for injection points in each borehole (view looking model north)

4.2 TAP advance

The tunnel excavation sequence proceeded according to the incremental excavations of the TAP. Each incremental excavation is shown in Figure 8. TAP advance was simulated for three cases:

- preconditioned model – pore pressure initialized in the DFN, faults, and HF planes;
- preconditioned model – pore pressure initialized in HF planes only; and
- un-preconditioned model.

The cumulative shear displacement on fractures (from beginning to end of the incremental excavation sequence) that directly correlates to the magnitude of the seismic events is shown in Figure 11 for the three investigated cases. The corresponding plot of event magnitude frequency for the three cases is shown in Figure 12.

The largest event magnitudes measured during TAP advance simulation before (Mw 1.71) and after preconditioning (Mw 0.58 when stimulating the DFN, faults, and HFs) are in good agreement with the actual event magnitudes recorded. The largest event magnitude recorded during the TAP advance was equal to approximately Mw 0.9. Using a dynamic friction angle scheme was key to matching field magnitude events in the model. The dynamic friction angle value (15°) used in the model is consistent with the findings by Brzovic et al. (2017) for large rockbursts at El Teniente Mine.

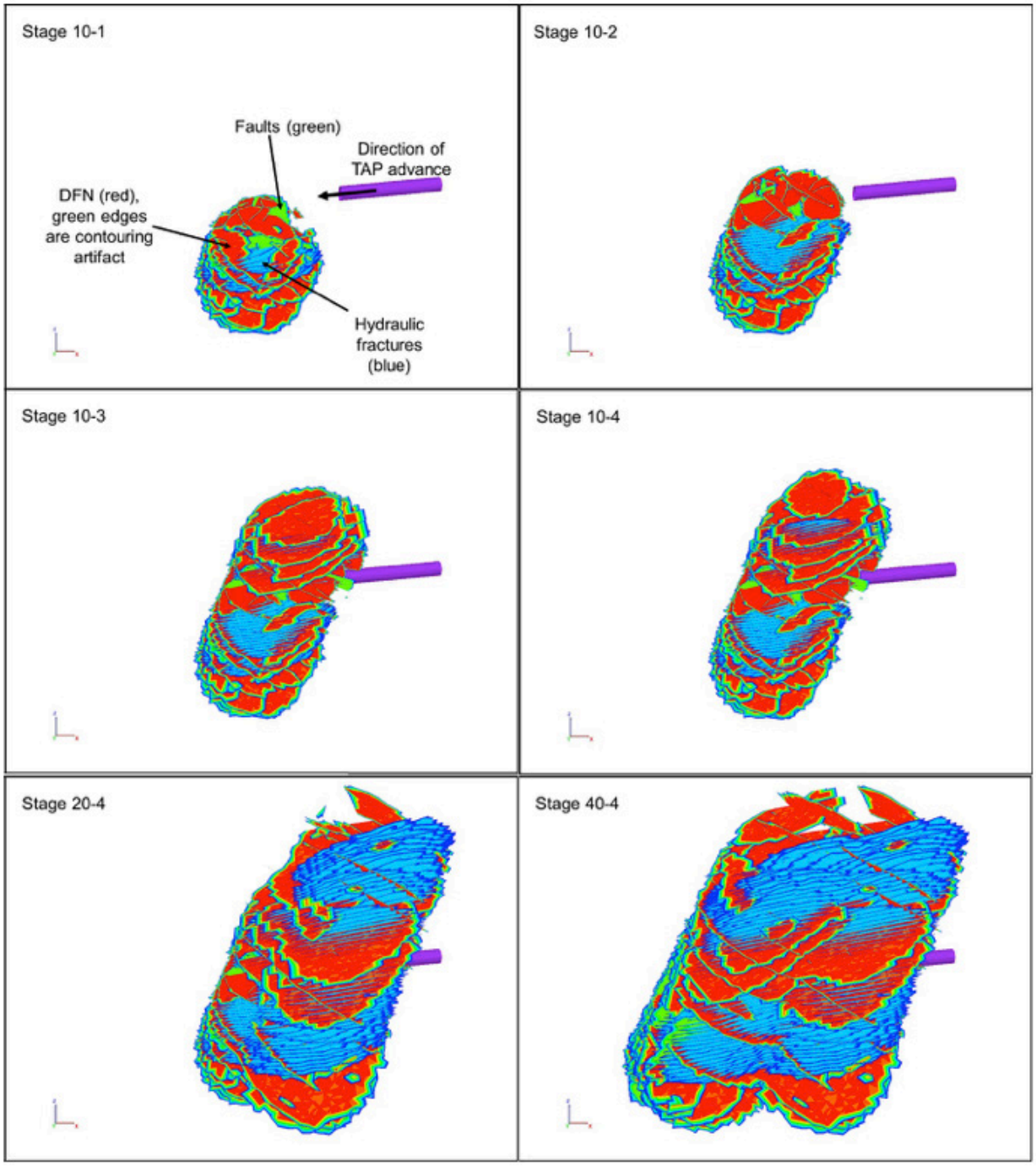

Figure 10 Stimulated discontinuities at different stages of HF treatment using the generalized scheme adopted from the local coupled model (view looking model north)

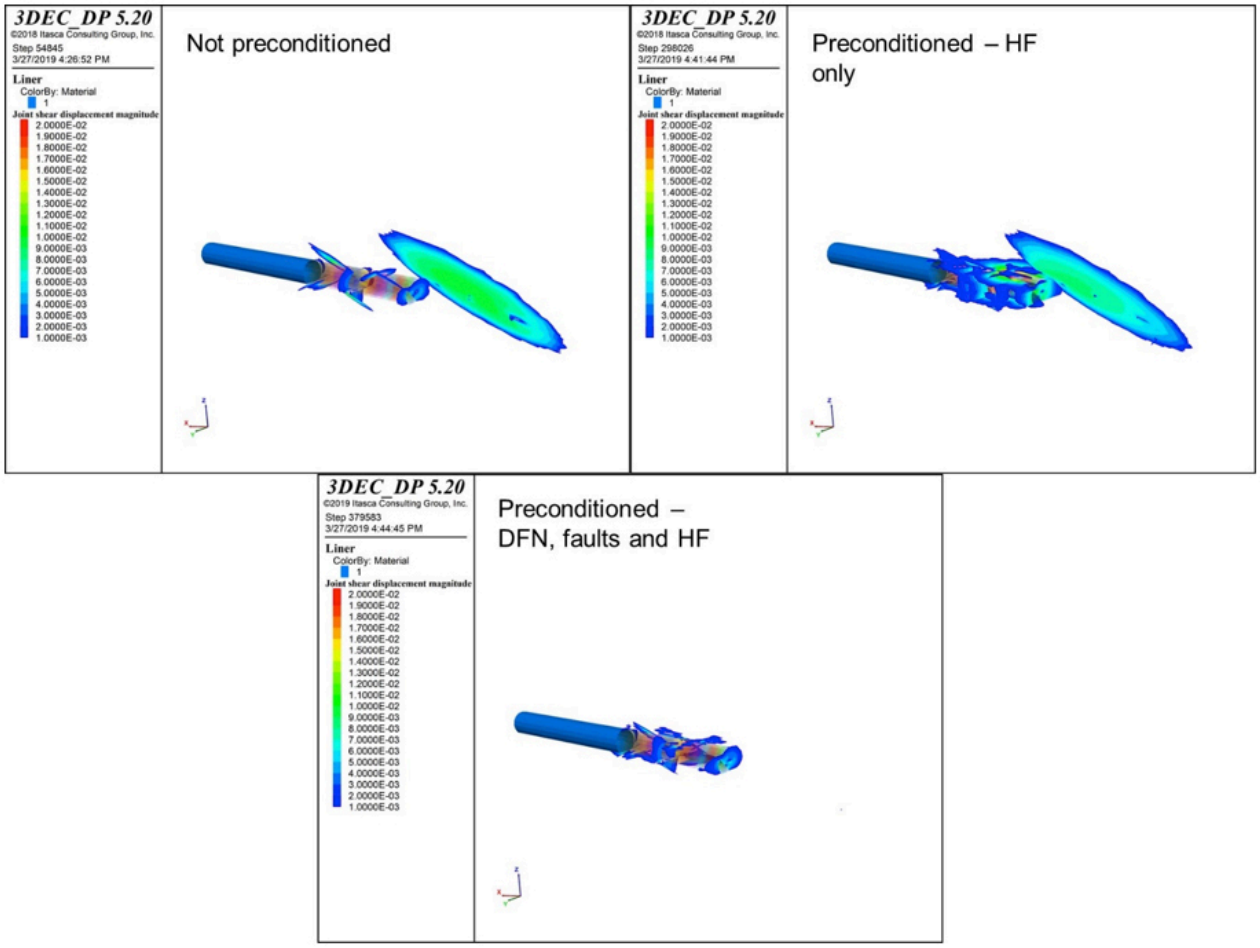

Figure 11 Contours of mining-induced shear displacements (m) on fractures at final stage of excavation (cumulative shear displacement from TAP excavation stages 1 to 16)

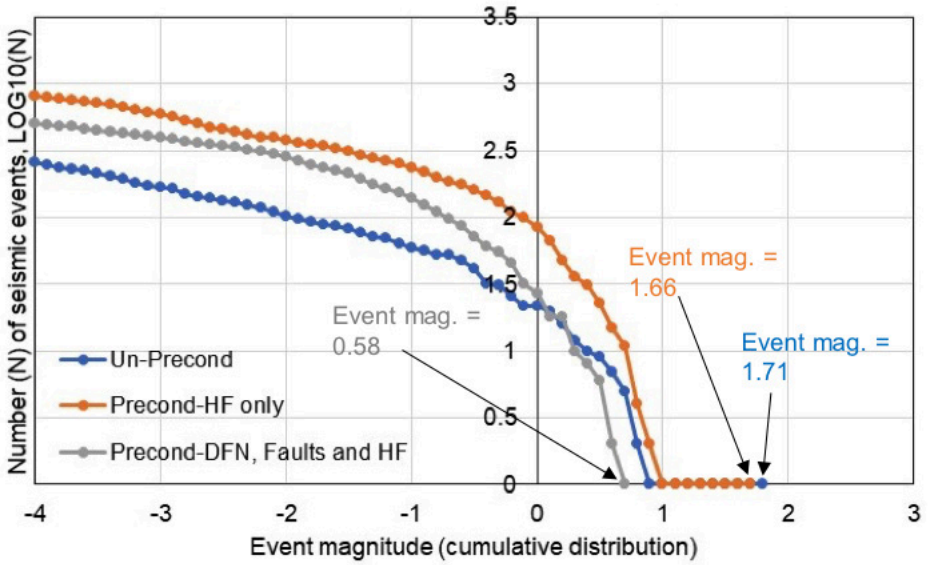

Figure 12 Event frequency versus magnitude for TAP advance before and after preconditioning

One mechanism that can cause seismicity during HF and reduce the potential for subsequent mining-induced seismicity is interaction between the hydraulic fracture and DFN, resulting in "hydro-shearing" on pre-existing fractures caused by fluid leakoff from the main hydraulic fracture. Basically, an increase in the pore pressure in pre-existing fractures causes a reduction of the effective stress and slip of those fractures. This process causes irreversible deformation in the rock mass (along pre-existing fractures) and local stress changes (i.e., relief of shear stresses on the fracture/fault plane under in-situ conditions), and can reduce the number of potential events and the magnitude of events caused by subsequent mining-induced stress changes. Schmidt & Eberhardt (2017) published results of a numerical study, conducted using UDEC (Itasca 2016), demonstrating that mechanism. Seismic response of the rock mass to TAP advance simulated before and after preconditioning (DFN, faults, and HF), shown in Figure 12, indicates the same trend. The magnitude of the largest event is shown to decrease from Mw 1.71 to Mw 0.58—a drastic improvement in reducing mining-induced seismic hazard. The contour of fracture shear displacement in Figure 11 implies the release of excess shear stress on marginally stable fractures by hydro-shearing during preconditioning. Preconditioning not only creates hydraulic fractures, but also reactivates DFN and faults. If the DFN and faults are not destressed by hydro-shearing, they can become unstable and slip during drift advance, generating large seismic events caused by stress perturbation.

It is interesting to notice the difference between the seismic behavior during TAP advance between the two preconditioned cases in Figure 12. In the case where preconditioning only assumes propagation of the isolated HF planes and disregards any interaction of those planes with the DFN, not only is the decrease in event magnitude insignificant (from Mw 1.71 to Mw 1.66), but also, on average, the mining-induced seismic hazard increases due to introducing new fractures to the rock mass. Although generally no shear stress is acting on HF planes considering only the far-field stress condition, the local stress changes ahead of and around the drift can cause slip and seismic events along those planes. In general, the seismic response of the preconditioned model with stimulated DFN, faults, and HF exhibits the anticipated behavior and is more consistent with the observations during the TAP advance (event magnitudes) as well as the seismic behavior reported by Morales et al. (2007) in contrast to the behavior reproduced by the HF-only preconditioned rock mass model. Therefore, the model results indicate that there is interaction between the hydraulic fractures and DFN and, consequently, there is a hydro-shearing effect on the critical stresses of pre-existing fractures during preconditioning.

5 Conclusions

This study confirms the beneficial effect of HF preconditioning for reducing mining-induced seismic hazard. It also verifies the role of hydro-shearing and the consequent release of excess shear stress on the marginally stable fractures as the main contributing factor to the reduction of mining-induced seismic hazard by HF treatment.

The close agreement of the seismic response predicted in the models with field observations confirms the successful calibration of the model. The calibration process involved fine-tuning the parameters related to in-situ stresses, discontinuity properties, and DFN simplification in a systematic way. The calibration of model parameters was performed as an iterative process with the goal of simultaneously matching the propagation pressure and seismicity. The field observations of HF-induced seismicity were matched in both the coupled and global models. The field observations of mining-induced seismicity were matched in the global model. It became apparent during the calibration process that it is essential to define a static and dynamic friction coefficient for discontinuities to numerically reproduce pre-mining stable conditions and to predict the large seismic event magnitudes observed during TAP advance. The calibrated model is a reliable tool for investigation of HF preconditioning and its potential benefit for other areas.

Acknowledgement

The authors acknowledge Codelco´s New Mine Level Project team for providing insights into the mine's ground behavior and the El Teniente Division management team for permission to publish this paper. This work was financed by Codelco and developed under a contract between Itasca and Codelco.

References

Blanksma, D, Damjanac, B & Lorig, L 2018, 'Effect of Hydraulic Fracturing Preconditioning on Mining-Induced Seismicity at Túnel Acceso Personal – Proof-of-Concept Study', Itasca report ICG 2-182607 to CODELCO.

Brzovic, A, Skarmeta, J, Blanco, B, Dunlop, R & Sepulveda, M 2017, 'Sub-horizontal faulting mechanism for large rockbursts at the El Teniente Mine,' in Proceedings, 9th International Symposium on Rockbursts and Seismicity in Mines, (November 2017, Santiago).

Ghazvinian, E, Damjanac, B & Lorig L 2019, 'Back-Analysis and Model Calibration of Hydraulic Fracturing Preconditioning at Túnel Acceso Personal', Itasca report ICG 2-1826-08:19R23 to CODELCO.

Itasca Consulting Group, Inc. 2016, 'UDEC — Universal Distinct Element Code. Minneapolis: Itasca'.

Itasca Consulting Group, Inc. 2015, '3DEC – Three-dimensional Distinct Element Code, Ver. 5.2. Minneapolis: Itasca'.

McGarr, A 1999, 'On relating apparent stress to the stress causing earthquake fault slip,' Journal of Geophysical Research: Solid Earth, vol. 104, pp. 3003-3011.

Morales, RF, Henriquez, JO, Molina, RE, Araneda, OA & Rojas, EG 2007, 'Rock Preconditioning Application in Virgin Caving Condition in a Panel Caving Mine CODELCO Chile El Teniente Division,' in Proceedings, Deep Mining 2007 (Fourth International Seminar on Deep and High Stress Mining, November 2007, Perth) pp. 111-120, Y. Potvyn, Ed. Perth: Australian Centre for Geomechanics.

Schmidt, ES & Eberhardt, E 2017, 'Numerical investigation of the use of hydraulic stimulation to mitigate fault slip risk in deep mines,' in Proceedings, Deep Mining 2017 (Eighth International Conference on Deep and High Stress Mining, March 2017, Perth) pp. 79–88, J. Wesseloo, Ed. Perth: Australian Centre for Geomechanics.

Verzani, LP, Russo, G, Grasso, P & Cabañas, A 2015, 'The Risk Analysis Applied to Deep Tunnels Design—El Teniente New Mine Level Access Tunnels, Chile,' In Engineering Geology for Society and Territory, vol. 6, pp. 1023-1030.